ISSN 0040-5795, Theoretical Foundations of Chemical Engineering, 2022, Vol. 56, No. 2, pp. 152–161. © Pleiades Publishing, Ltd., 2022.
Russian Text © The Author(s), 2022, published in Teoreticheskie Osnovy Khimicheskoi Tekhnologii, 2022, Vol. 56, No. 2, pp. 148–157.

Heat and Mass Transfer in a Dense Layer during Dehydration of Colloidal and Sorption Capillary-Porous Materials under Conditions of Unsteady Radiation-Convective Energy Supply

P. V. Akulich[a], * and D. S. Slizhuk[a]

[a] *Lykov Institute of Heat and Mass Exchange, National Academy of Sciences of Belarus, Minsk, Belarus*

**e-mail: akul@hmti.ac.by*

Received November 11, 2021; revised November 19, 2021; accepted December 3, 2021

Abstract—The results of numerical simulation and experimental study of heat and mass transfer in a stationary blown layer of colloidal capillary-porous materials of plant origin with cyclic radiation convective energy supply were presented. The mathematical model consists of the equations of gas phase mass conservation, filtration, and heat and mass transfer in phases, which allow for the internal resistance to heat and moisture transfer in particles when determining the heat and mass transfer coefficients. It includes the dependence of the specific heat of phase transition on particle moisture, particle shrinkage, and layer height during dehydration and the dependence of the effective coefficients of thermal conductivity of gas and vapor diffusion on the filtration rate. The results of modeling of dehydration of potato particles in a dense layer with cyclic radiation-convective energy supply were presented. It was shown that dehydration can be intensified and its duration can be reduced in comparison with the convective method. The calculated data were compared with the experimental data, confirming the adequacy of the model. The experimental kinetic dependences of desorption of activated carbon and zeolite with convective and radiation-convective energy supply were presented. The results of comparison indicate that the duration of desorption is markedly reduced when additional infrared irradiation is provided; for activated carbon, the process time is halved.

Keywords: heat and mass transfer in a fixed layer, radiation-convective drying, drying of plant materials

DOI: 10.1134/S0040579522020026

INTRODUCTION

Modern industries and technologies widely use the processes of drying, thermomechanochemical treatment, and modification of materials, which are generally characterized by high energy intensity and largely determine the quality of the final product and its cost. New applications of these processes constantly appear with the development of the economy. These technologies include the processing of materials of plant origin to obtain dry coarse or finely dispersed products and dehydration of materials in chemical industry, including regeneration of various sorbents. For drying of plant materials, convective units are most widely used, in which the specific heat consumption is rather large, reaching 6–8 MJ/kg of moisture and even higher. Methods used for intensification of heat and mass transfer processes include exposure to electromagnetic (infrared, microwave) radiation, evacuation of the medium, and the use of overheated vapor as a heat carrier [1–6].

The main difference and advantage of thermal radiation drying in comparison with convective drying are large specific (per unit area) heat fluxes. The optical properties of materials depend both on the properties of the dry framework and largely on the moisture content and forms of moisture binding, surface state, and other properties. The moisture content of a material has an ambiguous effect on its optical properties. The reflectivity decreases at increased moisture content for radiation with $\lambda = 1.4–15$ μm, which is caused by the significant absorptivity of water in this range of wavelengths [7]. For example, the depth to which IR radiation penetrates into a moist potato reaches 6 mm, while in a dry one it is 15–18 mm [8]. The depth of penetration of shortwave IR radiation into some foodstuffs reaches 7–30 mm [9]. However, the fraction of radiation energy penetrating even to a depth of 6 mm or more is relatively small. Due to high IR flux densities, the temperature of the surface layer of the irradiated material is usually higher than during convective drying, especially in the case of the removal of bound moisture. Plant materials are heat sensitive and lose quality when the temperature rises. Therefore, studies using unsteady cyclic action of energy fields are being further developed, which allow not only to intensify heat and mass exchange processes and increase their efficiency, but also to reduce the negative thermal effect. Recently, these methods of energy supply have

attracted the attention of researchers; they are being comprehensively studied and developed and used in new technologies and devices.

It was shown that preliminary IR irradiation of vegetable raw materials (e.g., apples, quinces, and melons) before drying reduces process duration and energy consumption by 25–35% and improves the quality of the final product, in particular, leads to a decrease in vitamin losses [10].

A study of oscillating infrared drying of seeds of vegetable crops (cucumbers, onions, etc.) was reported in [11]. It was shown that the use of this method at a seed temperature varied from 34°C to 40°C during the drying causes stimulation of seeds, which shows itself in an increase in their viability and germinating ability. The greatest stimulating effect is observed when the oscillating infrared drying lasts 40 min.

Pulsed infrared drying of thermolabile materials was proposed in the patent [12]. The method is characterized by a time-variant "heating–cooling" cycle with variable components of the heating and cooling stages. The temperature of the material is monitored with a non-contact pyrometer, and after the specified maximum and minimum temperatures of the material have been reached, the infrared emitters are switched on and off by means of a control device.

Review [13] provides a critical discussion of the use and comparative performance of IR radiation for drying some food materials, including grains, fruits, vegetables, and seafood. It was noted that radiation drying can be combined with convective, vacuum, and sublimation methods to increase the process rate and efficiency. A review of publications on the development of drying technologies (microwave, infrared, ultrasonic) for fruits and vegetables over the past five years was presented in [14]. It was noted that these drying methods provide higher process rate and thermal efficiency and improved quality of dried products (color, scent, texture, and nutrient retention) compared to conventional hot air drying. It was noted that further research and development in this area are needed.

The applicability and efficiency of infrared drying for fruits and vegetables with high water contents including kiwi, garlic, and various mushrooms was emphasized in [15]. It was noted that research is mainly aimed at optimizing the drying technology by varying the process time and temperature and combining various methods of energy supply to ensure high quality characteristics of products.

Kinetic and dynamic simulation of the drying process is performed using various approaches. Single particles are considered under conditions corresponding to the parameters in the drying chamber [16]. Heat and mass transfer in a dispersed layer of particles is modeled based on the continuum theory or Euler–Lagrange method, and statistical methods and percolation models are used. The applicability of the engineering method of chemical reactions and equilibrium activation energy for modeling infrared and other drying methods was assessed in [17]. Two-phase models of heat and mass transfer in a dense dispersed layer during convective and combined heating were presented in [18]. However, diffusion resistance in wet particles and their sorption properties were not taken into account. Modeling of the process of drying plant materials in a belt unit based on the equations of transfer and evaporation rate using the activation energy was considered in [19].

The goal of this study was to investigate the heat and mass transfer during dehydration of plant and sorption materials in a dense layer with an unsteady radiation-convective energy supply in order to examine the possibility of intensifying the process and increasing its efficiency.

THEORETICAL ANALYSIS

Problem formulation. The essence of the physical model of heat and mass transfer of wet material during unsteady radiation-convective treatment is as follows. A layer of dispersed colloidal capillary-porous material in a fixed state is considered (Fig. 2.1). It can move on a moving belt and be mixed. The layer is blown from bottom to top with a heat carrier (heated air) at a rate v_0. These methods of processing wet materials are used in convective belt, conveyor, and chamber shelf units. To intensify the heat and mass transfer, the dispersed layer is exposed on top to infrared radiation.

The radiation effect can be stationary or cyclic (impulse). In this case, stepwise or oscillating convective treatment is possible at different stages of processing. These modes are aimed at creating mild conditions of thermal exposure and reducing the specific heat consumption for moisture removal.

Mathematical model. The description of heat and mass transfer in a dispersed layer includes filtration, diffusion, desorption, binding energy of moisture with the material, phase transformation of the liquid, interfacial energy, mass exchange, thermal and diffusion resistance inside particles, and unsteady radiation-convective energy supply.

The model includes the following equations. The mass conservation equation of the gas phase is

$$\frac{\partial \rho_1}{\partial \tau} + \nabla \cdot (\rho_1 \mathbf{w}) = j_v. \quad (1)$$

The Darcy equation is

$$\mathbf{v} = -\frac{k}{\mu}\nabla p, \quad (2)$$

where $\mathbf{v} = \mathbf{w}\varepsilon$, $\mathbf{v}$ is the gas velocity calculated for the corresponding transverse section area of the disperse layer, i.e., filtration rate, m/s.

Then

$$\frac{\partial\left(\rho_l^\circ\varepsilon\right)}{\partial\tau}+\nabla\cdot\left(\rho_l^\circ\mathbf{v}\right)=j_v. \quad (3)$$

The equation of vapor transfer in the disperse (grain) layer:

$$\frac{\partial\left(\rho_v^\circ\varepsilon\right)}{\partial\tau}+\mathbf{v}\nabla\rho_v^\circ=\nabla\cdot\left(D_{v.\text{eff}}\nabla\rho_v^\circ\right)+j_v. \quad (4)$$

The equation of heat transfer in the gas phase of the layer:

$$c_l\rho_l^\circ\left(\varepsilon\frac{\partial T_l}{\partial\tau}+\mathbf{v}\nabla T_l\right)=\nabla\cdot\left(\lambda_{l\text{eff}}\nabla T_l\right)-\alpha S_{sp}\left(T_l-T_2\right). \quad (5)$$

The dependences of the effective heat conductivity coefficients of the gas phase and of vapor diffusion on the filtration rate were included in calculation using the following expressions in the direction of the corresponding axes: $\lambda_{ly.\text{eff}}=\lambda_l\left(\varepsilon+0.5\,\text{Pe}\right)$, $\lambda_{lx.\text{eff}}=\lambda_l\left(\varepsilon+0.1\,\text{Pe}\right)$, and $D_{v.\text{eff}}=D_v\varepsilon+0.5d_p\mathbf{v}$ [20, 21].

The equation of moisture transfer in the solid phase:

$$(1-\varepsilon)\frac{\partial U}{\partial\tau}=\nabla\cdot\left(D_{\text{eff}}\nabla U\right)-j_v. \quad (6)$$

If the layer of dispersed material is stationary, then the effective moisture diffusion coefficient is small and tends to zero. With forced mixing of the disperse layer, for example, with a horizontal stirrer, the effective diffusion coefficient within the framework of the diffusion model increases significantly. Its value along the layer height can be evaluated from the equation $D_{x.\text{eff}}=h^2/\tau_{cm}$, where τ_{cm} is the characteristic mixing time (characterizes the time within which the moisture concentration is leveled along the layer height). For the case of cyclic (impulse) mixing of the layer, the diffusion coefficient is a function of time.

The equation of heat transfer in the solid phase of the layer:

$$c_2\rho_d\left(1-\varepsilon\right)\frac{\partial T_2}{\partial\tau}=\nabla\cdot\left(\lambda_{2\text{eff}}\nabla T_2\right)+\alpha S_{sp}\left(T_l-T_2\right)-r_v j_v+\left(1-\varepsilon\right)I, \quad (7)$$

where $c_2=c_d+c_l u$.

The effect of layer mixing on the heat transfer by the disperse phase within the framework of the diffusion model can be taken into account by changing the effective thermal conductivity coefficient $\lambda_{2\text{eff}}$. The transfer processes in the gas phase depend on the layer mixing rate to a lesser extent, so its influence on these processes is neglected.

The intensity of mass transfer from solid to gas phase:

$$j_v=\beta_u S_{sp}\left[u-u_{\text{eql}}\left(p_v,T_l\right)\right]. \quad (8)$$

To describe the sorption (desorption) isotherms of the materials, the approximation formula is used [22]:

$$u_{\text{eql}}=u_{0.5}\left(T\right)\left(\frac{p_v}{p_s-p_v}\right)^{1/n}, \quad (9)$$

where $u_{0.5}\left(T\right)=A\exp\left[-B\left(T-T_0\right)\right]$ is the temperature dependence of the equilibrium moisture content at $\varphi=p_v/p_s=0.5$. The characteristic n is constant for the same material. As a result of approximation of the data of [23], for potatoes it is approximately $n=2.4$, and the constants are $A=0.135$, $B=0.0087$, $T_0=293$.

Diffusion moisture transfer in the particles of the material is included when determining the mass transfer coefficient. The latter is determined as the mass transfer coefficient that allows for the resistance of mass transfer from the particle surface and intradiffusion resistance to moisture transfer by the equation [24]

$$\beta=\left(\frac{1}{\beta'}+\frac{1}{\chi\beta''}\right)^{-1}, \quad (10)$$

where β'' is the coefficient of moisture diffusion, $\beta''=2\pi^2D/\left(3d_p\right)$.

The density of the gas mixture and water vapors is determined by the equation of state of the ideal gas: $\rho_l^\circ=pM_l/\left(R^*T_l\right)$ and $\rho_v^\circ=p_vM_v/\left(R^*T_l\right)$.

The amount of heat evolved in the particles of the material during IR irradiation is determined as

$$I=\delta(\tau)k'q_0\left(1-R_r\right)\exp\left[-k'\left(1-\varepsilon\right)\left(h-y\right)\right], \quad (11)$$

where $\delta(\tau)$ is the periodic (impulse) function of time.

The particles and the disperse layer are significantly deformed during the dehydration of colloidal capillary-porous materials. The volume, particle size, and height of the material layer decrease in this case.

The rate of motion of the material layer along the vertical coordinate due to shrinkage can be represented as [25]

$$v=\frac{dh}{d\tau}\frac{y}{h}=v_b\frac{y}{h},\quad v_b<0. \quad (12)$$

The rate of motion of the lower boundary of the layer at $y=0$ is zero, $v_r=0$, and the rate of the upper boundary is maximum, $v=v_b$. The motion of the upper boundary of the layer over the time τ is $\Delta h=h_0-h=v_b\tau y/h$, where $0\le\tau\le\tau_{c.sh}$, $\tau_{c.sh}$ is the time within which layer shrinkage is completed, whereafter it can be neglected. Shrinkage also occurs in the transverse (horizontal) direction along the x axis. In industrial apparatuses, however, the layer

height is usually much smaller than its width, and the heat carrier is blown in the vertical direction. Therefore, layer shrinkage along the horizontal axis has no significant effect on the heat and mass transfer and can be neglected in this problem.

The equation of moisture transfer in the solid phase for the two-dimensional case including layer shrinkage along the height can be represented as

$$(1-\varepsilon)\left(\frac{\partial U}{\partial \tau}+\mathrm{v}\frac{\partial U}{\partial y}\right)=\frac{\partial}{\partial x}\left(D_{x.\mathrm{eff}}\frac{\partial U}{\partial x}\right)+\frac{\partial}{\partial y}\left(D_{y.\mathrm{eff}}\frac{\partial U}{\partial y}\right)-j_{\mathrm{v}}. \quad (13)$$

The volume average current moisture content in the layer is determined by the equation

$$\bar{U}=\frac{1}{hl}\int_0^{h(\tau)}\int_0^{l}U(x,y,\tau)dxdy, \quad (14)$$

where l is the width of the disperse layer, m.

Accordingly, the equation of heat transfer in the solid phase is recorded as

$$c\rho_{\mathrm{c}}(1-\varepsilon)\left[\frac{\partial T_2}{\partial \tau}+\mathrm{v}\frac{\partial T_2}{\partial y}\right]=\frac{\partial}{\partial x}\left(\lambda_{2x.\mathrm{eff}}\frac{\partial T_2}{\partial x}\right)+\frac{\partial}{\partial y}\left(\lambda_{2y.\mathrm{eff}}\frac{\partial T_2}{\partial y}\right)+\alpha S_{\mathrm{sp}}(T_1-T_2)-r_{\mathrm{v}}j_{\mathrm{v}}+(1-\varepsilon)I. \quad (15)$$

The transfer processes in the gas phase depend on the layer deformation rate to a lesser extent; therefore, the effect of the deformation rate on these processes is neglected.

Shrinkage of the proper volume of raw potato particles was taken into account based on the experimental data according to the dependence $V=b_1u+b_2$, where V is the particle volume, m^3; $b_1=4.76\times10^{-8}$, $b_2=9.95\times10^{-8}$ are the empirical constants.

The decrease in the height of the disperse layer during dehydration was described by the empirical equation $h=b_3u+b_4$, where $b_3=0.0015$, $b_4=0.006$ are the empirical constants. The dependence of the layer height on the volumetric moisture content has the form $h=b_5U^2-b_6U+b_7$, where $b_5=8\times10^{-9}$, $b_6=1\times10^{-6}$, $b_7=0.0062$.

The rate of motion of the upper boundary is

$$v_{\mathrm{r}}=\frac{\partial U}{\partial \tau}(2b_5U-b_6). \quad (16)$$

The moisture conductivity coefficient is determined by the empirical equation [26]

$$D(u,T)=a_0\exp(-a_1/u)\exp(-a_2/T), \quad (17)$$

where $a_0=1.29\times10^{-6}$, $a_1=0.0725$, $a_2=2044$. Equation (17) is valid at parameters lying in the ranges $0.01<u<5$, $333<T<373$.

The specific heat of moisture evaporation is determined by the Clapeyron–Clausius equation:

$$r_{\mathrm{v}}=\frac{R^*T^2}{M_{\mathrm{v}}}\left(\frac{1}{p_{\mathrm{s}}}\frac{\partial p_{\mathrm{s}}}{\partial T}-\frac{nu_{0.5}^{n-1}}{u_{0.5}^n+u_{\mathrm{eq}}^n}\frac{\partial u_{0.5}}{\partial T}\right), \quad (18)$$

where $\partial u_{0.5}/\partial T=-Bu_{0.5}(T)$.

The pressure of the saturated water vapor p_{s} at temperatures from 0 to 100°C is determined by the approximate Antoine equation:

$$p_{\mathrm{s}}=133.3\times10^{8.074-\frac{1733}{t+233.84}}. \quad (19)$$

The diffusion coefficient of water vapor in air is $D_{\mathrm{v}}=D_0(p_0/p)(T/T_0)^{3/2}$, where $D_0=22\times10^{-6}$ m^2/s, $p_0=101325$ Pa, $T_0=273$ K.

The heat transfer coefficient in the stationary grain layer is determined by the equation [27]

$$\mathrm{Nu}_{\mathrm{eq}}=0.395\,\mathrm{Re}_{\mathrm{eq}}^{0.64}\,\mathrm{Pr}^{0.33}, \quad (20)$$

where $\mathrm{Re}_{\mathrm{eq}}=vd_{\mathrm{eq}}/\nu=4v/(S_{\mathrm{sp}}\nu)$.

The heat transfer coefficient is calculated with allowance for the thermal resistance of the heat conductivity of particles by the equation [23]

$$\alpha=\frac{1}{\frac{d_{\mathrm{eq}}}{\lambda_{\mathrm{p}}\,\mathrm{Nu}_{\mathrm{eq}}}+\frac{3}{2}\frac{d_{\mathrm{p}}}{\pi^2\lambda_{\mathrm{p}}}}. \quad (21)$$

In an assumption of similarity of the heat and mass transfer, the mass transfer coefficient is determined by the equation similar to (20).

The system of equations was solved under the following boundary conditions (Fig. 1). For the equation of mass conservation of the gas phase (3): $-\mathbf{n}\cdot\mathbf{v}\big|_{x=0;x=l}=0$; $-\mathbf{n}\cdot\mathbf{v}\big|_{y=0}=v_0$; $p\big|_{y=h}=p_0$. For the equation of vapor transfer (4): $\mathbf{n}\cdot\left(-D_{\mathrm{v.eff}}\nabla\rho_{\mathrm{v}}^{\circ}+\rho_{\mathrm{v}}^{\circ}\mathbf{v}\right)\Big|_{x=0;x=l}=0$ is the condition of impermeability; $\rho_{\mathrm{v}}^{\circ}\Big|_{y=0}=\rho_{\mathrm{v0}}^{\circ}$; $\mathbf{n}\cdot\left(-D_{\mathrm{v.eff}}\nabla\rho_{\mathrm{v}}^{\circ}\right)\Big|_{y=h}=0$. For the equation of heat transfer in the gas phase (5): $T_1\big|_{y=0}=T_{10}$, and $\mathbf{n}\cdot\left(-\lambda_{1\mathrm{eff}}\nabla T_1\right)\Big|_{y=h}=0$ other boundaries are heat-insulated. For the equations of moisture and heat transfer in the solid phase (6), (7) and (13), (15), respectively, $\mathbf{n}\cdot(-\lambda_{2\mathrm{eff}}\nabla T_2)\big|_{y=0;\ y=h}=0$ the boundaries are heat- and moisture-insulated.

Thus, a closed system of differential equations of heat and mass transfer in a stationary and stirred dispersed layer has been obtained, taking into account the above effects during unsteady radiation-convective energy treatment.

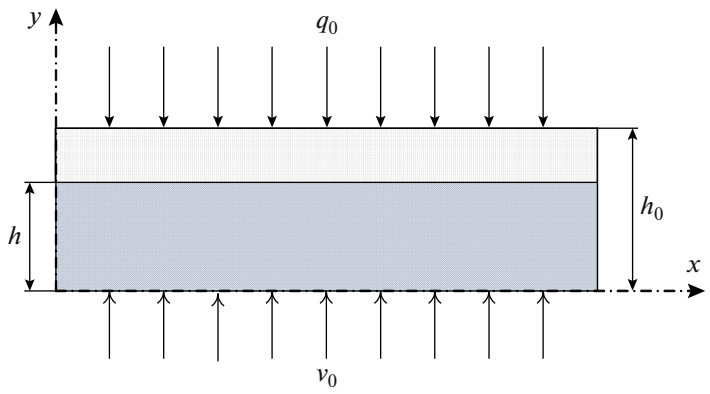

Fig. 1. To problem formulation.

RESULTS OF NUMERICAL SIMULATION AND COMPARISON WITH EXPERIMENTAL DATA

The heat and mass transfer in a fixed layer of potato particles of the Skarb variety was studied. The layer was blown with heated air from bottom to top. The particles were cubes with dimensions of ~7 × 7 × 7 mm. The wet material was placed on a reticular grid in two layers of particles, the initial layer height h_0 being ~14 mm. After shrinkage, the material particles were arranged in one row along the height. The disperse layer of the moist material was blown through with a heat carrier (heated air) at a low rate in the filtration mode. The air flow rate calculated for the layer section was ~0.5 m/s on the average, and its temperature at the inlet of the layer was 50–60°C. The radiant flux was directed to the material layer from above along the normal to it. To prevent overheating of the material by infrared radiation, the treatment was performed in a cyclic (pulse) mode in time. The mass of the layer was determined at specified time intervals. As a result, the kinetic curves of drying were obtained. For similar conditions, a numerical solution of the above system of equations was obtained using the Comsol program for non-stationary two-dimensional heat and mass transfer in a layer with allowance for the deformation (shrinkage) of particles and layer along the height during the radiation-convective energy supply.

The main parameters used in the calculations are: $k = 1\times10^{-8}$ m^2; $\mu_1 = 20\times10^{-6}$ Pa s; $c_1 = 1.006$ kJ/(kg K); $\lambda_1 = 0.029$ W/(m K); $D_{eff} = 5\times10^{-12}$ m^2/s; $R^* = 8314.2$ J/(kmol K); $M_v = 18.02$ kg/kmol; $\rho_d = 175$ kg/m^3; $u_0 = 5.2$ kg/kg; $U_0 = 910$ kg/m^3 of the solid phase; $S_{sp} = 428.6$ m^2/m^3; $v_0 = 0.5$ m/s; $h_0 = 0.014$ m; $T_{10} = 333$ K; $q_0 = 8.8\times10^3$ W/m^2; $R_r = 0.05$; $k' = 220$; $\varepsilon = 0.5$.

Figure 2 clearly shows that the cyclic effect of infrared radiation on the disperse layer of the material leads to an increase in the rate of dehydration and a reduction in its duration compared to the convective method due to the intensification of heat and mass transfer processes. A comparison of the results of numerical simulation with experimental data indicates that they agree satisfactorily. Marked discrepancy is observed during the first period of the process. This is evidently because of nonuniform gas distribution over the layer section in the experimental study due to the small height of the material layer. The shape of the dehydration curve with a large proportion of the period of the falling rate indicates that the effect of intradiffusion moisture transfer on process duration is dominant.

The moisture content of particles along the layer height during dehydration differs insignificantly. The

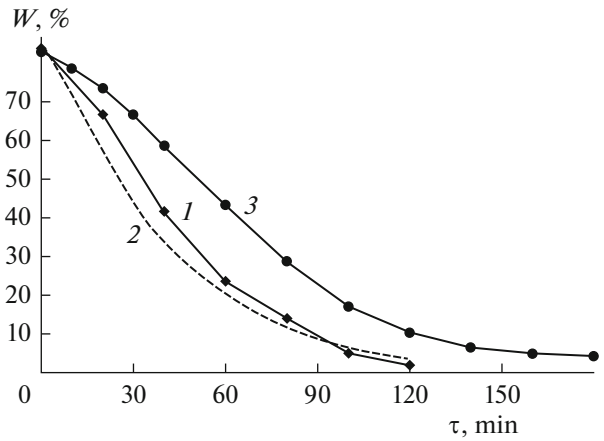

Fig. 2. Kinetic dependences of dehydration of raw potato particles during convective and radiation-convective energy supply in the blown layer: (*1*) cyclic radiation-convective energy supply: time ~0–20 min, $(\tau_{ir} + \tau_{ps}) \times$ number of cycles: (2 + 1) × 6; ~20–40 min: (1 + 2) × 6 and further convective heat supply; (*2*) calculated curve; (*3*) convective energy supply. $t_1 = 60$°C, $v = 0.5$ m/s; initial layer height $h_0 = 14$ mm.

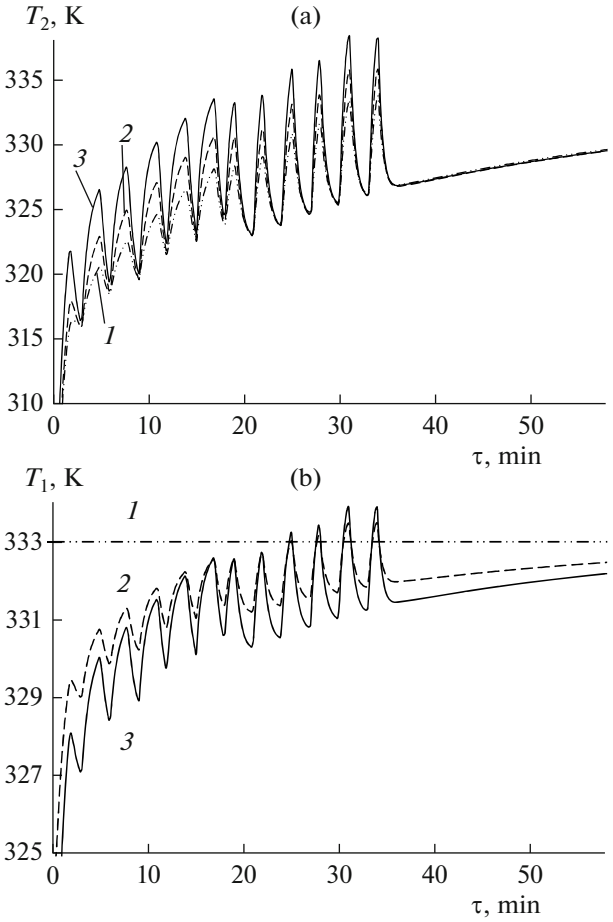

Fig. 3. (a) Time dependences of particle temperature in the disperse layer: (*1*) $y = 0$; (*2*) $y = 0.5h$; (*3*) $y = h.x = 0.06$ m. (b) Time dependences of the gas temperature in the disperse layer: (*1*) $y = 0$; (*2*) $y = 0.5h$; (*3*) $y = h.x = 0.06$ m.

moisture content of particles in the upper region of the layer decreases slightly faster in the first period.

At the initial moment of time, the disperse layer has a uniform temperature distribution of particles $t_2 = 20$°C. Due to the radiative and convective energy supply, the layer is heated faster than the convective heat supply. The temperature of particles in the layer fluctuates with an increase in amplitude over time (Fig. 3).

At the start of the process, during the IR treatment periods, the temperature of the particles does not reach the maximum allowable temperature, and only after layer heating and reduction in the moisture content, the particle temperature in the cycles increases, but is short-term. As can be seen, during the periods when IR radiation is turned off, the particle temperature quickly decreases and tends toward the temperature of the wet thermometer or gas. After 30–40 min of irradiation, the layer temperature increases rapidly; therefore, it is reasonable to use cyclic (pulse) exposure. Note that, to prevent overheating of particles, the duration of irradiation periods was reduced after the heating of the layer. During the periods of infrared exposure, the temperature of particles in the upper regions of the layer is higher than in its lower regions (Fig. 4).

However, this difference is insignificant. The greatest difference is observed when the layer is heated. The layer temperature decreases markedly during cooling, differing insignificantly along the layer height. The layer height decreases appreciably because of particle shrinkage, which can be seen from the change in the vertical coordinate y.

The gas temperature at the inlet of the layer was set constant and equal to $t_1 = 60$°C. Figure 3 shows that

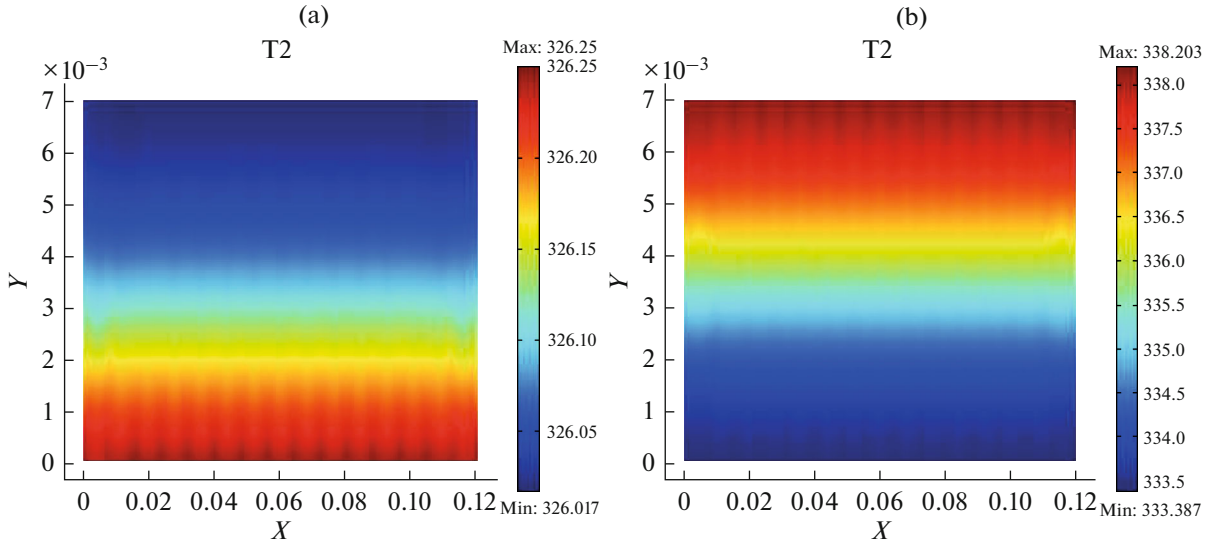

Fig. 4. (a) Temperature field of the solid phase of the disperse layer in the cooling cycle at $\tau = 1970$ s. (b) Temperature field of the solid phase of the disperse layer in the cooling cycle at $\tau = 2030$ s.

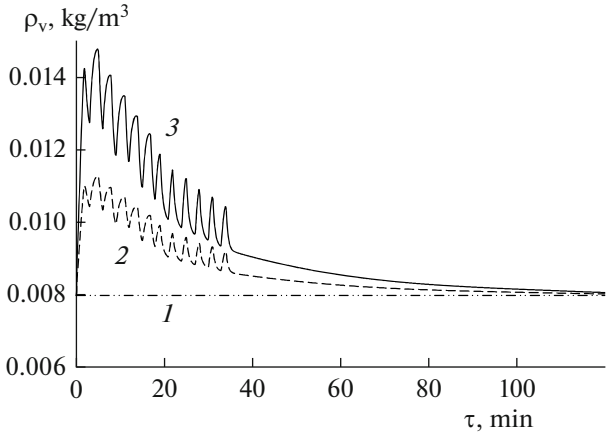

Fig. 5. Time dependences of water vapor concentration in the disperse layer: (*1*) $y = 0$; (*2*) $y = 0.5h$; (*3*) $y = h$. $x = 0.06$ m.

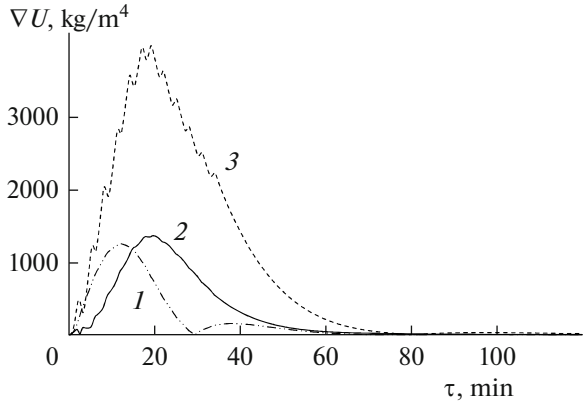

Fig. 6. Time dependences of moisture content gradient in the disperse layer: (*1*) $y = 0$; (*2*) $y = 0.5h$; (*3*) $y = h$. $x = 0.06$ m.

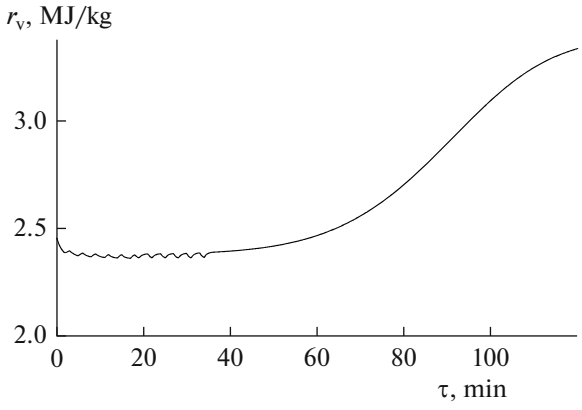

Fig. 7. Time dependence of the specific heat of evaporation.

the temperatures of the gas and particles inside the disperse layer have similar periodic dependences. The gas temperature on the layer surface is lower than in the middle of the layer at the start of the process and then becomes higher. The maximum gas temperature during active periods of irradiation is slightly lower than the particle temperature.

The concentration of water vapor increases rapidly in the initial period of the process and becomes higher in the upper sections of the layer. It decreases with time and fluctuates, tending toward the value at the inlet of the layer (Fig. 5).

Interesting time dependences were obtained for the moisture concentration gradient in the disperse phase, which have a maximum (Fig. 6).

The maximum increases significantly on passing to the upper layers (curve *3*) and shifts to the region of longer times. The moisture content gradient affects the deformation of particles and is of interest for problems in which this circumstance is important.

Figure 7 shows that the specific heat of evaporation of bound moisture changes markedly with time due to a decrease in the moisture content of particles. At the start of the process, it slightly decreases, which is caused by an increase in the particle temperature. When the bound moisture is removed, the specific heat of evaporation noticeably increases due to the binding energy of moisture with the material. As the moisture content of particles along the layer height differs insignificantly, the heat of evaporation also changes slightly along the vertical coordinate.

Studies of shrinkage of the disperse layer (Fig. 8a) indicate that the layer height changes mainly during the removal of free moisture. Further, the change in layer height is not so significant. Figure 8b shows the change in the volume of particles depending on their moisture content. The experimental data were approximated by a linear dependence. It can be seen that the layer height and the particle volume significantly decrease during dehydration, which should be taken into account when modeling such processes.

The kinetics of drying of activated carbon and CaX zeolite sorption materials were studied experimentally. The drying (desorption) processes take place during regeneration of activated carbon used for water purification. In drying technologies, granular zeolite is used for air drying; it should be regenerated by desorption. Desorption of materials was performed by the radiation-convective method as follows. The diameter of spherical particles of activated carbon lies in the range 1–2.2 mm, while cylindrical granules of zeolite have a diameter of ~3 mm and a height of 4–5 mm. The wet material was poured onto a reticular grid in the form of a layer of small height. The height of the activated carbon layer was ~5 mm, and that of the zeolite layer was ~7 mm. During convective desorption, the material layer was blown with heated air with a temperature of 150°C at the inlet. The air filtration rate was ~0.2 m/s.

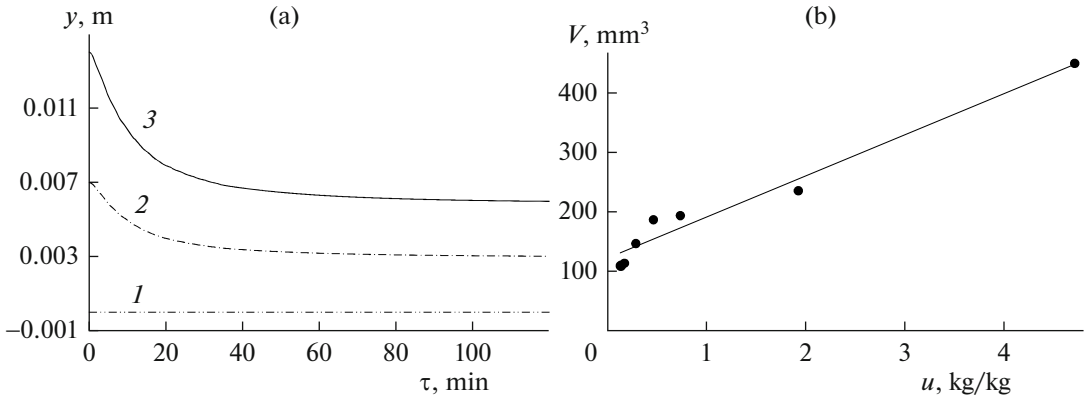

Fig. 8. (a) Dependences of shrinkage of the disperse layer: (*1*) $y = 0$; (*2*) $y = 0.5h$; (*3*) $y = h$. (b) Dependences of particle shrinkage.

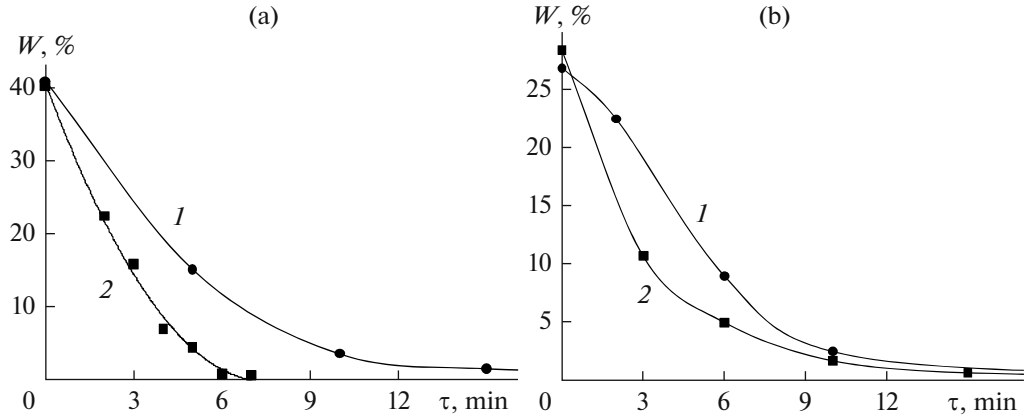

Fig. 9. (a) Experimental kinetic dependences of desorption of activated carbon: (*1*) convective heat supply; (*2*) radiation-convective energy supply. (b) Experimental kinetic dependences of desorption of zeolite: (*1*) convective heat supply; (*2*) radiation-convective energy supply.

With radiation-convective energy supply, the layer of wet material was blown through with air heated to 150°C and irradiated from above with infrared radiation. The emitter was an ICH-101 ceramic heater (Nomacon). The emitter power was 1 kW; the surface temperature ~690°C; the distance of the emitter from the layer 300 mm. The kinetic dependences for the indicated methods of energy supply are shown in Fig. 9.

A comparison shows that infrared irradiation of a layer of material can significantly reduce the duration of desorption (it is halved for activated carbon in this mode).

The radiation-convective method of desorption can be used for regeneration of sorbents during air drying in drying units, including for materials of plant origin.

CONCLUSIONS

As a result of numerical simulation and experimental studies, the dependences of the kinetics of dehydration and shrinkage of particles, heat and mass transfer in a fixed layer of colloidal capillary-porous materials of plant origin were established using raw potato particles as an example with convective and cyclic radiation-convective energy supply. The calculated data agree with the experimental data. It was shown that dehydration can be significantly intensified and its duration reduced.

The kinetic dependences of desorption of activated carbon and zeolite with convective and radiation-convective energy supply were obtained experimentally. A comparison of the dependences indicates that the duration of desorption with additional infrared irradiation was significantly reduced; in particular, for activated carbon, the duration is halved.

NOTATION

c	specific heat capacity, J/(kg K)
c_d, c_l	specific heat capacity of dry particles and liquid, J/(kg K)

d_p, d_{eq}	equivalent diameter of particles and channels, m
h	height of the material layer, m
k	permeability coefficient of a layer of particles, m^2
k'	absorbance
M	molecular mass, kg/kmol
p_v	partial pressure of water vapor in the layer, Pa
q_0	flux density of incident IR radiation on the layer surface, W/m^2
r_v	specific heat of evaporation, J/kg
R^*	gas constant, J/(kmol K)
R_r	reflection factor
R_v	gas constant for water vapor, J/(kg K)
S_{sp}	specific surface area of the layer, m^2/m^3
T	temperature, K
u	moisture content of particles, kg/kg, $u = U/\rho_c$
U	volumetric moisture content of a particle, kg/m^3
$\mathbf{v}$	gas filtration rate, m/s
$\mathbf{w}$	gas rate in gaps between layer particles, m/s
W	moisture content of the material, kg of moisture/ kg of wet material or %
x and y	horizontal and vertical coordinates, m
α	heat transfer factor, $W/(m^2 K)$
$\beta_u = \beta_p \Delta p_v/\Delta u$	mass transfer factor divided by the difference between moisture contents, $kg/(m^2 s\ kg/kg)$
$\beta_p = \beta/(R_v\bar{T})$	mass transfer factor divided by the difference between the partial pressures of vapor, $kg/(m^2 s\ Pa)$
β'	mass transfer factor divided by the difference between concentrations, $kg/(m^2 s\ kg/m^3)$
ε	layer porosity
$\chi = \rho_l/\rho_v$	equilibrium ratio of densities of liquid and vapor
λ	heat transfer coefficient, W/(m K)
μ_v	dynamic coefficient of vapor viscosity, Pa s
ρ_l° and ρ_l	true and reduced density of the gas phase (dry air and water vapor), kg/m^3, $\rho_l = \varepsilon\rho_l^\circ$
ρ_2 and ρ_d	density of moist and dry particles, kg/m^3
τ	time, s
τ_{ir}, τ_{ps}	irradiation time and pause in the cycle, s
Re_{eq}	Reynolds number
$Nu_{eq} = \alpha' d_{eq}/\lambda_l$, $Nu'_{eq} = \beta d_{eq}/D_v$	heat and diffusion Nusselt numbers
$Pr = \nu/a$	Prandtl number

SUBINDICES AND SUPERINDICES

0	initial state
1 and 2	gas and solid phases
s	saturated state
v	vapor
eql	equilibrium state
p	particle
eq	equivalent
eff	effective
–	averaging sign

REFERENCES

1. Akulich, P.V., *Calculation of Dryers and Heat Exchangers*, Minsk: Belaruskaya Navuka, 2010.
2. Akulich, P.V. and Akulich, A.V., *Convective Dryers: Methods and Examples of Calculation*, Minsk: Vysheishaya Shkola, 2019.
3. Akulich, P.V. and Slizhuk, D.S., Heat and moisture transfer in dispersed fixed bed of plant materials in combined energy supply, *Inzh.-Fiz. Zh.*, 2020, vol. 93, no. 4, p. 800.
4. Nesterov, A.V., *Industrial Drying*, St. Peterburg: Lan', 2022.
5. Teplyashin, V.N., Chentsova, L.I., and Nevzorov, V.N., *Technologies and Equipment for Drying of Plant Raw Materials: A Study Guide*, Krasnoyarsk: Krasnoyarsk. Gos. Agrar. Univ., 2019.
6. Kumar, C., Microwave-convective drying of food materials: A critical review, *Crit. Rev. Food Sci. Nutr.*, 2019, vol. 59, no. 3, p. 379.
7. Ginzburg, A.S., *Foundations of Theory and Technology of Food Drying*, Moscow: Pishchevaya Promyshlennost', 1973.
8. Atanazevich, V.I., *Food Drying: A Reference Book*, Moscow: DeLi, 2000.
9. Ginzburg, A.S., *IR Equipment in Food Industry*, Moscow: Pishchevaya Promyshlennost', 1966.
10. Snezhkin, Yu.F., Boryak, L.A., and Izbasarov, D.S., Energy saving and intensification of pulsed infrared drying, *Prom. Teplotekh.*, 2001, vol. 23, nos. 4–5, p. 90.
11. Rudobashta, S.P., Zueva, G.A., and Zuev, A.I., Oscillating infrared drying and stimulation of seeds, in *Pro-*

ceedings of the XV Minsk International Forum on Heat and Mass Transfer, Minsk, May 23–26, 2016, vol. 3, p. 191.

12. Grigor'ev, I.V. and Rudobashta, S.P., RF Patent no. 2393397 C2 RU (2009).
13. Sakare, P., Prasad, N., Thombare, N., Singh, R., and Sharma, S.C., Infrared drying of food materials: Recent advances, *Food Eng. Rev.*, 2020, vol. 12, p. 381.
14. Li, K., Zhang, M., Mujumdar, A.S., and Chitrakar, B., Recent developments in physical field-based drying techniques for fruits and vegetables, *Drying Technol.*, 2019, vol. 37, no. 15, p. 1954. https://doi.org/10.1080/ 07373937.2018.1546733
15. Zartha Sossa, J.W., Orozco, G.L., García Murillo, L.M., Peña Osorio, M., and Sánchez Suarez, N., Infrared drying trends applied to fruit, *Front. Sustain. Food Syst.*, 2021, vol. 5, Article 650690. https://doi.org/10.3389/fsufs.2021.650690
16. Rudobashta, S.P., Kartashov, E.M., and Zueva, G.A., Heat and mass transfer in drying of a plate in a continuous high- and superhigh-frequency electromagnetic field, *Theor. Found. Chem. Tekhnol.*, 2021, vol. 55, no. 2, p. 261.
17. Putranto, A. and Chen, X.D., Reaction engineering approach modeling of intensified drying of fruits and vegetables using microwave, ultrasonic and infrared-heating, *Drying Technol.*, 2020, vol. 38, nos. 5–6, p. 747. https://doi.org/10.1080/07373937.2019.1708750
18. Kalender'yan, V.A. and Boshkova, I.L., *Heat and Mass Transfer in Apparatuses with Dense Bed of Dispersed Material*, Kiev: Izdatel'skii Dom "Slovo", 2011.
19. Sorokovaya, N.N., Snezhkin, Yu.F., Shapar', R.A., and Sorokovoi, R.Ya., Mathematical modeling and optimization of continuous drying of thermolabile materials, *Inzh.-Fiz. Zh.*, 2019, vol. 92, no. 5, p. 2218.
20. Amiri, A. and Vafai, K., Analysis of dispersion effect and non-thermal equilibrium, non-Darcian, variable porosity incompressible flow through porous media, *Int. J. Heat Mass Transfer*, 1994, vol. 37, no. 6, p. 939.
21. Baikov, V.I. and Pavlyukevich, N.V., *Thermodynamics and Statistical Physics: A Study Guide*, Minsk: Vysheishaya Shkola, 2018.
22. Gorobtsova, N.E., Method of description and calculation of sorption–desorption isotherms, general for various materials, in *Teplomassoobmen-VI: Proceedings of the VI All-Union Conference on Heat and Mass Transfer*, Minsk, 1980, vol. VIII, p. 60.
23. Grishin, M.A., Atanazevich, V.I., and Semenov, Yu.G., *Food Product Dryers*, Moscow: Agropromizdat, 1989.
24. Frank-Kamenetskii, D.A., *Diffusion and Heat Transfer in Chemical Kinetics*, Moscow: Nauka, 1987.
25. Rudobashta, S.P., Kartashov, E.M., and Zueva, G.A., Mathematical modeling of convective drying of materials with taking into account their shrinking, *Inzh.-Fiz. Zh.*, 2020, vol. 93, no. 6, p. 1446.
26. Sablani, S., Rahman, S., and Al-Habsi, N., Moisture diffusivity in foods—An overview, in *Drying Technology in Agriculture and Food Sciences*, Ed. by Arun S. Mujumdar, Enfield (NH), USA: Science Publishers, Inc., 2000, pp. 35–39.
27. Aerov, M.E., Todes, O.M., and Narinskii, D.A., *Apparatuses with Stationary Granular Bed*, Leningrad: Khimiya, 1979.

Translated by L. Smolina